Variation in the microbiome of the spider mite *Tetranychus truncatus* with sex, instar, and endosymbiont infection

Yu-Xi Zhu, Zhang-Rong Song, Shi-Mei Huo, Kun Yang and Xiao-Yue Hong*

Department of Entomology, Nanjing Agricultural University, Nanjing, Jiangsu 210095, China

*Author for correspondence:

Xiao-Yue Hong;

E-mail: xyhong@njau.edu.cn;

Fax: +86 25 84395339.

Running Head: Microbiome of spider mites

ABSTRACT

Most arthropod-associated bacterial communities play a crucial role in host functional traits, whose structure could be dominated by endosymbionts. The spider mite *Tetranychus truncatus* is a notorious agricultural pest harboring various endosymbionts, yet the effects of endosymbionts on spider mite microbiota remain largely unknown. Here, using deep sequencing of the 16S rRNA gene, we characterized the microbiota of male and female *T. truncatus* with different endosymbionts (*Wolbachia* and *Spiroplasma*) across different developmental stages. Although the spider mite microbiota composition varied across the different developmental stages, Proteobacteria were the most dominant bacteria harbored in all samples. Positive relationships among related OTUs dominated the significant coassociation networks among bacteria. Moreover, the spider mites coinfected with *Wolbachia* and *Spiroplasma* had a significantly higher daily fecundity and juvenile survival rate than the singly infected or uninfected spider mites. The possible function of spider-mite associated bacteria was discussed. Our results highlight the dynamics of spider mite microbiotas across different life stages, and the potential role of endosymbionts in shaping the microbiota of spider mites and improving host fitness.

Keywords: spider mite, microbiome, *Wolbachia*, *Spiroplasma*, fitness

INTRODUCTION

Most arthropods harbor diverse bacterial communities in their bodies (Adair *et al.* 2018; Brinker *et al.*, 2019). Associations between insect hosts and microbiomes impact host ecology and evolution (Frago, Dicke, and Godfray 2012). It is well known that the arthropod-associated microbiome provides the most crucial services, such as impacting development and reproduction (Duron *et al.* 2008), aiding in the digestion of food (Feldhaar 2011; Hansen and Moran 2014), providing protection against natural enemies or pathogens (Oliver *et al.* 2003; Scarborough, Ferrari, and Godfray 2005), supplying key nutrients (Douglas 1998) and improving tolerance to abiotic stresses (Dunbar *et al.* 2007). These functions could be impaired by broad changes in the arthropod-associated microbiome. Understanding the dynamics of microbiota is essential for unraveling the complex interplay between arthropods and their bacterial symbionts. However, the dynamics and the ecological factors shaping these communities are not well understood.

The microbial community of arthropods is influenced by the sex and life stages of the host. The sex of the host has been documented to profoundly affect bacterial microbiota composition in mosquitoes (Diptera: Culicidae) (Minard, Mavingui, and Moro 2013), ticks (*Ixodes scapularis*) (Thapa, Zhang, and Allen 2018), and other arthropods (Martinson, Douglas, Jaenike 2017; Fromont, Adair, and Douglas 2019). Across different developmental stages, ants (*Nasutitermes arborum*) (Diouf *et al.* 2018), bees (*Megalopta centralis* and *M. genalis*) (McFrederick *et al.* 2014), thrips (*Hoplothrips carpathicus*) (Kaczmarczyk *et al.* 2018) and mosquitoes (*Aedes aegypti*) (Audsley *et al.* 2018) exhibit distinct bacterial community structures. The red palm weevil gut microbiota displays a highly stable microbial community with low variance in abundance through different life stages (Muhammad *et al.* 2017).

Heritable endosymbionts are another important factor that affects microbiota composition in many arthropods (Audsley *et al.* 2018; Fromont, Adair, and Douglas 2019; Kolasa *et al.* 2019; Brinker *et al.* 2019). *Wolbachia* are widespread heritable endosymbionts of arthropods (> 65% of species) known for their profound effects on host fitness (Sazama, Ouellette, and Wesner 2019) that can influence microbiota composition in many arthropods

(Brinker *et al.* 2019). For example, Audsley *et al.* (2018) reported that *Wolbachia* infection alters the relative abundance of resident bacteria in adult *A. aegypti*. Dittmer and Bouchon (2018) determined that feminizing *Wolbachia* influence microbiota composition in *Armadillidium vulgare*. In addition to *Wolbachia*, *Rickettsia* infection of the flea (*Ctenocephalides felis*) and tick (*I. scapularis*) can also alter the species richness of their associated microbiomes (Pornwiroon *et al.* 2007; Thapa, Zhang, and Allen 2018). These studies indicated that the endosymbionts shape the overall diversity of the microbiome. However, some studies have suggested that the abundance of *Wolbachia* does not affect the composition of the microbiota in *Drosophila melanogaster* (Adair *et al.* 2018). The effect of endosymbionts on the host microbiota appears to be closely related to host species identity. Spider mites (Acari: Tetranychidae) are widely occurring arthropod pests on crops that harbor a diversity of endosymbionts (Walter and Proctor, 1999; Zhang *et al*. 2016; Zélé *et al.* 2018a), however, it is unclear whether the endosymbionts alter the spider mite microbiome.

Among spider mites, *Tetranychus truncatus* is the most economically important species and became the dominant pest in China in 2009 (Jin *et al.* 2018). This species undergoes five gradual developmental stages: egg, larva, protonymph, deutonymph, and adult (Walter and Proctor, 1999). *T. truncatus* harbors a wide variety of the vertically transmitted endosymbionts, including *Wolbachia*, *Cardinium*, and *Spiroplasma*, which manipulate host reproduction via various phenotypic effects (Zhu *et al.* 2018; Zhang *et al.* 2018). Endosymbiont infection patterns of *T. truncatus* can exhibit large variation in space and time and are affected by numerous factors, such as host genotype (Zhang *et al.* 2016), feeding status and environmental factors (Zhu *et al.* 2018). Given that multiple endosymbiont infections are frequently observed in the natural populations of *T. truncatus*, it is of great interest to investigate whether the presence of endosymbionts impacts spider mite microbiomes and performance. Our previous study indicated that host plants and antibiotics can shape *T. truncatus* bacterial communities and that bacterial symbionts can improve mite performance (Zhu *et al.* 2019a). However, whether endosymbiont infection, sex, and life stage affect spider mite microbiomes and its associated functions is poorly understood.

In this study, we used a high-throughput 16S rRNA amplicon sequencing procedure to investigate the microbiotas of male and female *T. truncatus* with different endosymbionts (*Wolbachia* and *Spiroplasma*) across developmental stages. Furthermore, we performed bioassays to assess the effect of bacterial symbionts on the fitness of spider mite hosts. The results indicated that the diversity of spider mite microbiotas varies according to sex,

developmental stage, and the endosymbiont infection status and highlight the potential function of the microbiota in host performance and fitness.

METHODS AND MATERIALS

Spider mite samples and endosymbiont infection status

Spider mites

Four spider mite (*T. truncatus*) strains with different infection patterns were established: infection of mites with both *Wolbachia* and *Spiroplasma* (designated as *w*+*s*+), *Wolbachia* only (*w*+), *Spiroplasma* only (*s*+) or no symbionts (*w*-*s*-). Three strains (*w*+*s*+, *w*+ and *s*+) were originally collected from Shenyang, Liaoning Province, China. The *w*-*s*- individuals were obtained by raising *s*+ strains on common bean placed on a cotton bed soaked in tetracycline solution (0.1%, w/v) for three generations as described by Zhang *et al.* (2018). To eliminate the potential effects of the tetracycline, the *w*-*s*- strains were reared on untreated detached bean leaflets for at least 15 generations before they were used for the bacterial infection status and mite fitness tests (Fig. 1).

To obtain spider mite strains with a similar genetic background, introgressive backcrossing was used to homogenize the nuclear genetic backgrounds of infected and uninfected spider mites, following the method described by Turelli and Hoffmann (1991). Briefly, approximately 40 uninfected males (*w*-*s*-) were collected to mate with a cohort of approximately 20 females of each four spider mite strains (*w*+*s*+, *w*+, *s*+ and *w*-*s*-) to guarantee sufficient mating. Then, in subsequent generations, uninfected males were mated to each of the four introgressed spider mites strains progeny for 7 generations, and the four spider mite strains were cultured for approximately 22 generations before being used in the experiments (Fig. 1).

All spider mites used in these experiments were reared on leaves of common bean (*Phaseolus vulgaris* L.) placed on a water-saturated sponge mat in a Petri dish at 25 ± 1°C and 60% relative humidity and under 16 h light: 8 h dark conditions. To control the age of the tested spider mites, adult spider mite females were placed on a bean leaf inside a Petri dish, where they laid eggs for 24 h. These Petri dishes were then kept under controlled conditions until the spider mites developed into adulthood.

Endosymbiont infection status

For each of the spider mite strains, the infection status was checked during the experiment as described by Zhang *et al.* (2018). Briefly, DNA was extracted from individual mites using the QIAGEN DNeasy Kit (Germany) according to the manufacturer's protocol. All DNA samples were first PCR screened for the mitochondrial gene COI as a quality control (Navajas *et al.* 1996). *Wolbachia* and *Spiroplasma* presence was detected using PCR amplification of wsp and 16S rRNA, respectively. Each reaction was carried out on a Veriti instrument (ABI Biosystems, U.S.) in a 25 μl volume containing 12.5 μl of 2× Taq Master Mix (Vazyme Biotech, China), 0.5 μl of primer (20 μmol/L each), and 1 μl of DNA extract. Positive and negative controls were included in the PCRs.

Spider mite performance

To determine the effect of the endosymbionts on the performance of *T. truncatus*, we measured the life history traits of individuals from the four spider mite strains. A single 2 ± 1-day-old female (since the last molt) was placed on a bean leaf disc (diameter ca. 1.5 cm), with 30 leaf discs per spider mite strain. After 4 days of oviposition, the live females were transferred to new leaf discs for another 4 days. The number of eggs produced by each spider mite strain was recorded using a stereo microscope. The eggs on the leaf discs were checked daily to evaluate hatchability. This experiment was repeated three times. Significant differences in the fecundity, and juvenile survival among the four spider mite strains were identified with Kruskal-Wallis tests. The log-rank (Mantel-Cox) test was used to compare the percent female survival among the four spider mite strains.

DNA extraction and 16S rRNA gene amplicon sequencing

DNA extraction

Two hundred eggs, 200 larvae, 100 protonymphs, 50 deutonymphs, 20 adult females, and 20 adult males from each of the four spider mite strains (*w+s+*, *w+*, *s+*, and *w-s-*) were pooled to form one sample, with four biological replicates per sample. Each sample was collected in a 1.5 ml collection tube filled with 75% (v/v) ethanol using a sterile soft-bristle brush. All samples were stored at -20 °C until DNA extraction.

Total genomic DNA from the pooled spider mite samples was extracted using the QIAGEN DNeasy Kit (Germany) as described above. Before extraction, each sample was cleaned with75% ethanol and sterile dH_2O.

16S rRNA gene amplicon sequencing

The V3-V4 region of the 16S rRNA gene was amplified using the primer pair 341F (5'-CCTAYGGGRBGCASCAG-3') and 806R (5'-GGACTACNNGGGTATCTAAT-3'). The cycling conditions for this PCR step were as previously described (Zhu *et al.* 2019a). Negative controls for DNA extraction were conducted using sterile water; no amplified PCR products were detected. The resulting amplicons were extracted from 2% agarose gels and purified using the AxyPrep DNA Gel Extraction Kit (Axygen Biosciences, Union City, CA, U.S.) according to the manufacturer's instructions and quantified using QuantiFluor™-ST (Promega, U.S.). Purified PCR products were quantified with Qubit®3.0 (Life Invitrogen), and 24 amplicons with different barcodes were equally mixed. The pooled DNA product was used to construct an Illumina paired-end library following Illumina's genomic DNA library preparation procedure. Then, the amplicon library was paired-end (2 × 250 bp) sequenced on an Illumina HiSeq 2500 platform (Shanghai Biozeron Co., Ltd.) using standard protocols.

Sequence assembly

Raw fastq files were first demultiplexed using in-house Perl scripts according to the barcode sequence information for each sample with the following criteria: (i) the 250 bp reads were truncated at any site receiving an average quality score < 20 over a 10 bp sliding window, discarding the truncated reads that were shorter than 50 bp; (ii) exact barcode matching, 2 nucleotide mismatch in primer matching, reads containing ambiguous characters were removed; and (iii) only sequences overlapping by more than 10 bp were assembled according to their overlap sequence. Reads that could not be assembled were discarded.

UPARSE (version 7.1 http://drive5.com/uparse/) was used to cluster OTUs according to a 97% similarity cutoff, and chimeric sequences were identified and removed using UCHIME. The phylogenetic affiliation of each 16S rRNA gene sequence was analyzed with the RDP Classifier (http://rdp.cme.msu.edu/) against the SILVA (SSU132)16S rRNA database using a confidence threshold of 70%.

Statistical and bacterial community analyses

All statistical analyses were performed in R ver. 3.3.1 (R Development Core Team, 2016) and MicrobiomeAnalyst (https://www.microbiomeanalyst.ca/) (Dhariwal *et al.* 2017).

The alpha diversity of each sample was calculated according to the number of observed OTUs and the Chao 1, ACE (abundance-based coverage estimator), Shannon, Fisher, and Simpson diversity indexes. To assess the variation in diversity measures among spider mites among the different developmental stage/sex and endosymbiont combinations, we used generalized linear models (GLMs) with a binomial distribution. The effects of the different factors were assessed using two- way ANOVA. The variance attributed to the endosymbionts was set as the random error in the GLM, with DS (developmental stage and sex) as a fixed factor.

To identify differences in the microbial communities among the different samples, the permutational multivariate analysis of variance (PERMANOVA) was performed based on the Bray-Curtis dissimilarity distance matrices. Multivariate relationships among the microbiotas of the different samples were visualized with principal coordinates analysis (PCoA) ordination plots.

Two approaches were used to assess the relationships among members of the spider mite microbiota. First, cooccurrence patterns among pairs of bacterial OTUs were assessed using MicrobiomeAnalyst (Dhariwal *et al.* 2017). When the expected frequency of two OTUs co-occur more or less than observed, if the distributed randomly, was < 0.05, that OTU pair was considered to have significant positive or negative cooccurrence, respectively. Second, a coassociation network was inferred from the read counts for bacterial OTUs with the sparse inverse covariance estimation for the ecological association inference method (Kurtz *et al.* 2015).

The Phylogenetic Investigation of Communities by Reconstruction of Unobserved States (PICRUSt) (http://picrust.github.io/picrust/tutorials/genome_prediction.html) program based on the Kyoto Encyclopedia of Genes and Genomes (KEGG) database was used to predict the functional alteration of the microbiotas across the different samples. The obtained OTU data were used to generate BIOM files formatted as input for PICRUSt v1.1.09 with the make. biom script usable in mothur. OTU abundances were mapped to Greengenes OTU IDs as input to speculate about the functional alteration of the microbiotas. Kruskal-Wallis tests were used to compare the KEGG ortholog (KO) abundances of the four spider mite strains.

RESULTS

Illumina sequencing output

A total of 2959518 sequences were obtained from the 90 samples sequenced for bacterial 16S rRNA gene amplicons using an Illumina HiSeq platform, with an average of 32,883 sequences per sample after quality filtering and removal of chimeric sequences. All the sequences were classified into 59 OTUs (> 0.1% of all sequences) at 97% sequence identity, which belonged to 5 phyla, 19 orders, 28 families and 37 genera (Fig. S1). Good's coverage for each sample was more than 99.9% (Table S1). Overall, most of the sequences obtained from the bacterial communities associated with the *T. truncatus* strains belonged to Proteobacteria (87.58%), followed by Actinobacteria (5.35%), Firmicutes (4.06%), and Bacteroidetes (2.91%) (Fig. S1 and S2).

Microbiota community variation among the four spider mite strains at different life stages

The diversity of the spider mite bacterial communities, as indicated by the Shannon index, was significantly affected by the endosymbiont infection status (log-rank (LR) *Chi-square*: 10.354; *df* = 3; *P* = 0.0158), DS (LR *Chi-square*: 112.515; *df* = 5; *P* < 0.001), and the interaction between these variables (LR *Chi-square*: 33.791; *df* = 15; *P* = 0.0036; Fig. 2; Table 1). At the genus level, the relative abundances of *Sphingomonas* (OTU 1), *Rudaea* (OTU 4), *Sphingobium* (OTU 6), *Achromobacter* (OTU 9), *Caulobacter* (OTU 12), *Bosea* (OTU 19), *Sphingopyxis* (OTU 30), *Methylobacterium* (OTU 35), *Stenotrophomonas* (OTU 41), and *Bacteroides* (OTU 51) in endosymbiont-infected female strains (*w*+*s*+, *w*+ and *s*+) were higher than those in uninfected female strains (*w*-*s*-) (Table S2). However, these bacteria were more abundant in uninfected male strains (*w*-*s*-) than in endosymbiont-infected male strains (*w*+*s*+, *w*+ and *s*+) (Table S2). In addition, the relative abundances of *Sediminibacterium* (OTU 15), *Bosea* (OTU 19), *Tsukamurella* (OTU 28), and Methylobacterium (OTU 35) in the four spider mite strains tended to decrease during the transition from egg to adult, while the relative abundance of *Egicoccus* (OTU24) tended to increase (Table S2).

The PCoA based on Bray-Curtis distances explained 76.9% of the variance in microbiota composition, with PC1=33.5%, and PC2=31% (Fig. 3). There were significant differences in

the microbiotas associated with the four spider mite strains across different developmental stages (PERMANOVA: $F = 7.164$; R-squared: 0.714; $P < 0.001$; Fig. 3).

Although the relative abundances of microbial taxa varied across the spider mite strains at different developmental stages, there were several shared microbes across all samples (Fig. 4). The family *Sphingomonadaceae* was dominated, representing ~40% of the assemblage across all developmental stages. Eleven OTUs (11/51 = 21.57%) were detected in all samples, and thus represent a core set of spider mite microbes (Table S2, Fig. S3).

Microbial cooccurrence and coassociation network

Our analysis of relationships among bacterial taxa in spider mites was conducted on the OTUs detected in all samples. Only 100 (16.81%) of the 595 pairwise comparisons showed statistically significant cooccurrence, comprising 43 (7.23%) positive and 57 (9.58%) negative relationships (Table S3, Fig. 5). Most bacterial taxa were not involved in either predominantly positively or negatively cooccurring pairs.

In the coassociation network, nodes correspond to OTUs and edges represent significant coassociation between the two OTUs. The coassociation network revealed more positive than negative coassociation (Fig. S4). The results indicated that coassociations among microbial OTUs are predominantly positive.

Functional inference

The spider mite-associated bacterial symbionts contain genes involved in staurosporine biosynthesis, lipid metabolism, glutathione metabolism, carbohydrate metabolism, and membrane transport (Table 2). The main functions were similar among the four spider mite strains at different developmental stages (Table 2). There were significant differences among the larvae of the four spider mite strains in terms of bacteria rich in genes involved in FADH2 O2-dependent halogenase I (Kruskal-Wallis test: *Chi-square* = 8.88; *df* = 3; $P = 0.03$), a LacI family transcriptional regulator (*Chi-square* = 8.72; *df* = 3; $P = 0.03$), iron complex outermembrane receptor protein (*Chi-square* = 9.38; *df* = 3; $P = 0.02$), methyl-accepting chemotaxis protein (*Chi-square* = 8.65, *df* = 3, $P = 0.03$), and acetyl-CoA C-acetyltransferase (*Chi-square* = 8.60; *df* = 3; $P = 0.04$) (Table 2). However, genes involved in 3-oxoacyl-[acyl-carrier protein] reductase, RNA polymerase sigma-70 factor, and glutathione S-transferase did not significantly different among the four spider mite strains across developmental stages (Table 2).

Impact of endosymbionts on spider mite performance

There were significant differences in daily fecundity (Kruskal-Wallis test: *Chi-square* = 27.86; *df* = 3; $P < 0.0001$), and juvenile survival rate (*Chi-square* =52.69; *df* = 3; $P < 0.0001$) among the four spider mite strains (Fig. 6a, b). The spider mite strain *w+s+* showed significantly higher daily fecundity and juvenile mortality than the other three spider mite strains (Fig. 6a, b). There were no significant differences in the female survival rate among the four spider mite strains (LR test: *Chi-square* = 3.182; *df* = 3; $P = 0.3644$; Fig. 6c).

DISCUSSION

Spider mites are notorious agricultural pest species worldwide. They harbour both endosymbionts and a microbiota, which can potentially interact and affect spider mite life history traits. In this study, we characterized microbiota variation across various development stages in four spider mite strains of *T. truncatus* that differ in their endosymbiont composition.

Microbiota variation among different spider mite strains

A key result of this study is that the microbiota of *T. truncatus* was influenced by the sex, and developmental stage of host. The male and female adult *T. truncatus* exhibited a distinct microbial community structures despite having the same rearing environment. The relative abundances of the genera *Arthrobacter*, *Acinetobacter*, *Tsukamurella*, and *Bacteroides* in female spider mites were higher than that in males. Similarly, research on *Drosophila* sp. has also shown that the microbiota may be affected by the sex of the host (Martinson, Douglas, Jaenike 2017; Fromont, Adair, and Douglas 2019). In some cases, male and female insects exhibit different ecological behaviors in terms of nutritional and dispersal capabilities, and the nutrient composition of food sources may directly impact the diversity of the bacteria present (Walter and Proctor, 1999). Additionally, the microbiota of many insects varies across host life stages (Andongma *et al.* 2015; Audsley *et al.* 2018; Muhammad *et al.* 2017; Ali, Abrar, Hou 2019). During metamorphosis, the structure of the microbiota changes drastically in the transition between life stages (Tchioffo *et al*. 2016). Here, the relative abundances of *Sediminibacterium*, *Bosea*, *Tsukamurella*, and *Methylobacterium* in spider mites tended to decrease during the transition from egg to adult, but the relative abundance of *Egicoccus* tended to increase. The dynamic changes in the microbial profiles of spider mites

might be attributed to shifts in gut physiological conditions, such as gut bacterial metabolism-mediated variations in pH. The transmission patterns of different bacteria species may also affect their presence in different life stages.

In addition to sex and developmental stage, the presence/absence of heritable endosymbionts can influence the diversity of the microbiota of spider mites. A similar pattern has been described in *A. aegypti*, and *A. vulgare*, where infection by the endosymbiont *Wolbachia* alters the microbiota composition in the host (Audsley *et al*. 2018; Dittmer and Bouchon 2018; Kolasa *et al*. 2019). There are at least two hypotheses that might explain how endosymbionts can affect the microbiota in hosts. The first is that the endosymbionts may compete for limited space and resources with other bacteria in the host body, which would result in the exclusion of the least competitive symbionts (Audsley *et al*. 2018). Another explanation is that endosymbionts may negatively affect the density or transmission of several bacteria, resulting in the absence of some bacteria during the transmission process (Kondo, Shimada, Fukatsu 2005; Goto, Anbutsu, and Fukatsu 2006). However, at this stage, it is not clear which of these hypotheses applies to the results found in this study. In contrast, previous studies of *D. melanogaster* and *Anopheles stephensi* (Adair *et al*. 2018; Chen *et al*. 2016) found that the endosymbionts do not affect the composition of the microbiota. These results indicate that the endosymbionts shaping the microbiome may strongly depend on host species, and this may be interpreted as host-species specificity.

Although microbiota composition differs strongly among insects species, Proteobacteria and Firmicutes appear to be the most prevalent phyla in various invertebrates, including *Octodonta nipae* (Ali, Abrar, Hou 2019), *A. albopictus* and *A. aegypti* (Zouache *et al*. 2011), *Bactrocera dorsalis* (Andongma *et al.*, 2015), *Rhynchophorus ferrugineus* (Muhammad *et al*. 2017), and *D. melanogaster* (Adair *et al*. 2018). Here, we found that Proteobacteria are the most dominant bacteria harbored in *T. truncatus*, which is consistent with previous findings for *T. urticae* (Staudacher et al. 2017), *T. phaselus*, *T. kanzawai*, and *T. ludeni* (Zhu *et al*. 2019b). These results indicate that the dominant taxa are consistently present and may play an important role in host functional traits.

Functional analysis of the spider mite microbiota

Functional predictions show that the *T. truncatus*-associated bacteria are mainly related to staurosporine biosynthesis, lipid metabolism, glutathione metabolism, carbohydrate metabolism, and membrane transport. We found differences in these categories among the different developmental stages and strains of spider mites, suggesting that the microbiota

could have important functions at specific developmental stages across the different spider mite strains. In most cases, the main functional characteristics of the microbiota were similar among four spider mite strains across the different developmental stages. The results indicate that bacterial functional stability occurs in spider mites despite the high microbial composition variability across different developmental stages. The specific symbiotic bacteria of arthropods can play vital roles in host functional traits (Gurung, Wertheim, and Falcao Salles 2019). Some members of the spider mite microbial community, such as *Pantoea*, *Enterobacter*, and *Pseudomonas*, have the potential to change and manipulate anti-herbivore plant response, as shown in Colorado potato beetles (*Leptinotarsa decemlineata*) (Chung *et al*. 2013), false potato beetles (*L. juncta*) (Wang *et al*. 2016), and fall armyworms (*Spodoptera frugiperda*) (Acevedo *et al*. 2017). In *Psacothea hilaris*, *Lactococcus* bacteria are involved in the production of lactic acid and polysaccharides digestion (Mazza *et al.*, 2014). *Acinetobacter* bacteria can degrade pesticides for their insect hosts (Hao *et al*., 2002), and *Enterococcus* present in the gut of *R. ferrugineus* have been shown to have the ability to degrade cellulose (Muhammad *et al*. 2017). Bacteria including *Lactococcus, Acinetobacter*, and *Enterococcus* were also detected in spider mites. It would be interesting to experimentally test whether these bacteria play the same role in spider mites. It is of prime importance to investigate the specific functions of taxa to unravel the complex interplay between spider mites and their symbionts.

The effect of endosymbionts on mite fitness

In nature, the endosymbionts *Wolbachia* and *Spiroplasma* are widespread in spider mite species (Zhang *et al*. 2016; Zélé *et al*. 2018a) and can affect key aspects of the host, including host fecundity and fitness (Zhang *et al*. 2018; Zélé *et al*. 2018b). A previous study by our lab showed that *Wolbachia* and *Spiroplasma* affect the fecundity and fitness of *T. truncatus* (Zhang *et al*. 2018; Zhu *et al*. 2019a). In a parallel study, we observed that the spider mite strains coinfected with *Wolbachia* and *Spiroplasma* have a significantly higher the daily fecundity and juvenile survival rate than the singly infected or uninfected spider mite strains. Symbiont-conferred reproduction and fitness benefits can favor their host occurrence (Zhang *et al.* 2018), which could partially explain why spider mites can undergo outbreaks and have become the dominant pest in recent years in China. Furthermore, a recent study found that microbiome interactions in the insects shape host fitness (Gould *et al.* 2018). We found that positive relationships, mostly among related OTUs, dominated both the significant cooccurrences and coassociation networks among bacteria, indicative of interdependence between bacteria. These findings raise the possibility that the interactions between these

bacteria play an important role in shaping spider mite performance or fitness, not only endosymbionts.

Notably, we used antibiotics to generate spider mite strains uninfected with *Wolbachia* and *Spiroplasma*. Although the spider mites were reared on detached bean leaflets without antibiotics for at least 15 generations before they were used for the subsequent experiment, we cannot rule out the effects of the antibiotic treatment on the microbiotas of the spider mites. Another unexpected result was that OTU 31 (*Wolbachia*) was much less abundant in the *w+* than in the *w+s+* strain. Moreover, OTU 396 (*Spiroplasma*) showed overall low abundance in both *w+s+* and *s+* strains. This could indicate that the experimental manipulation of endosymbiont composition in minuscule arthropods is difficult. Conversely, it also shows that the reliable assessment of a microbiome member, which occurs at low abundance is difficult with the current methods at hand (Zhou *et al.* 2015; Pollock *et al.* 2018). Thus, further research is required to assess the microbiota in natural populations of spider mites using next-generation sequencing approaches according to the recommendations of Eisenhofer *et al.* (2019). This would help to detect and validate the presence of rare members of the microbiome.

In conclusion, this study provides a comprehensive overview of the microbiota in spider mites varying in sex, instar, and endosymbionts and shows the potential function of the microbiota in many key aspects of spider mites, especially in host fitness. The results will allow a better understanding of the complex interaction between spider mites and their bacterial symbionts.

SUPPLEMENTARY DATA

Supplementary data may be found online in the supporting information tab for this article.

ACKNOWLEDGMENTS

We are grateful to Xiao-Feng Xue and Jing-Tao Sun for their valuable comments on an earlier version of this manuscript.

FUNDING

This study was supported by the National Natural Science Foundation of China (31672035, 31871976, and 31901888) and the China Postdoctoral Science Foundation (2019M651864).

Conflicts of interest. None declared.

REFERENCES

Acevedo FE, Peiffer M, Tan CW, *et al*. Fall armyworm-associated gut bacteria modulate plant defense responses. *Mol Plant Microbe In* 2017; 30(2): 127-137.

Adair KL, Wilson M, Bost A, *et al*. Microbial community assembly in wild populations of the fruit fly *Drosophila melanogaster*. *ISME J* 2018; 12 (4): 959.

Ali H, Abrar M, Hou Y. Pyrosequencing uncovers a shift in bacterial communities across life stages of *Octodonta nipae* (Coleoptera: Chrysomelidae). *Front Microbiol* 2019; 10: 466.

Andongma AA, Wan L, Dong YC, *et al*. Pyrosequencing reveals a shift in symbiotic bacteria populations across life stages of *Bactrocera dorsalis*. *Sci Rep-UK* 2015; 5: 9470.

Audsley MD, Seleznev A, Joubert DA, *et al*. *Wolbachia* infection alters the relative abundance of resident bacteria in adult *Aedes aegypti* mosquitoes, but not larvae. *Mol Ecol* 2018; 27(1): 297–309.

Brinker P, Fontaine MC, Beukeboom LW, *et al*. Host, symbionts, and the microbiome: the missing tripartite interaction. *Trends Microbiol* 2019; 27 (6): 480-488.

Chen S, Zhao J, Joshi D, *et al*. Persistent infection by *Wolbachia* wAlbB has no effect on composition of the gut microbiota in adult female *Anopheles stephensi*. *Front Microbiol* 2016; 7: 1485.

Chung SH, Rosa C, Scully ED, *et al*. Herbivore exploits orally secreted bacteria to suppress plant defenses. *P Natl Acad Sci USA* 2013; 110(39): 15728-15733.

Dhariwal A, Chong J, Habib S, *et al*. MicrobiomeAnalyst: a web-based tool for comprehensive statistical, visual and meta-analysis of microbiome data. *Nucleic Acids Res* 2017; 45(W1): W180–W188.

Diouf M, Miambi E, Mora P, *et al*. Variations in the relative abundance of *Wolbachia* in the gut of *Nasutitermes arborum* across life stages and castes. *FEMS Microbiol Lett* 2018; 365 (7): fny046.

Dittmer J, Bouchon D. Feminizing *Wolbachia* influence microbiota composition in the terrestrial isopod *Armadillidium vulgare*. *Sci Rep-UK* 2018; 8(1): 6998.

Douglas AE. Nutritional interactions in insect- microbial symbioses: Aphids and their symbiotic bacteria *Buchnera*. *Annu Rev Entomol* 1998; 43: 17–37

Dunbar HE, Wilson ACC, Ferguson NR, *et al*. Aphid thermal tolerance is governed by a point mutation in bacterial symbionts. *PLoS Biol* 2007; 5: 1006–1015

Duron O, Bouchon D, Boutin S, *et al*. The diversity of reproductive parasites among arthropods: *Wolbachia* do not walk alone. *BMC Biol* 2008; 6: 27.

Eisenhofer R, Minich JJ, Marotz C, *et al*. Contamination in low microbial biomass microbiome studies: issues and recommendations. *Trends Microbiol* 2019; 27:105-117.

Feldhaar H. Bacterial symbionts as mediators of ecologically important traits of insect hosts. *Ecol Entomol* 2011; 36 (5): 533–543.

Frago E, Dicke M, Godfray HCJ. Insect symbionts as hidden players in insect–plant interactions. *Trends Ecol Evol* 2012; 27 (12): 705–711.

Fromont C, Adair KL, Douglas AE. Correlation and causation between the microbiome, *Wolbachia* and host functional traits in natural populations of drosophilid flies. *Mol Ecol* 2019; 28 (7):1826-1841.

Goto S, Anbutsu H, Fukatsu T. Asymmetrical interactions between *Wolbachia* and *Spiroplasma* endosymbionts coexisting in the same insect host. *Appl Environ Microb* 2006; 72: 4805– 4810.

Gould AL, Zhang V, Lamberti L, *et al.* (2018). Microbiome interactions shape host fitness. *P Natl Acad Sci USA* 2018, 115(51): E11951-E11960.

Gurung K, Wertheim B, Falcao Salles J. The microbiome of pest insects: it is not just bacteria. *Entomol Exp Appl* 2019; 167(3): 156-170.

Hansen AK, Moran NA. The impact of microbial symbionts on host plant utilization by herbivorous insects. *Mol Ecol* 2014; 23: 1473–1496.

Hao OJ, Kim MH, Seagren EA, *et al*. Kinetics of phenol and chlorophenol utilization by *Acinetobacter* species. *Chemosphere* 2002; 46: 797–807.

Jin PY, Tian L, Chen Lei, *et al*. Spider mites of agricultural importance in China, with focus on species composition during the last decade (2008–2017). *Syst Appl Acarol* 2018; 23(11): 2087–2098.

Kaczmarczyk A, Kucharczyk H, Kucharczyk M, *et al*. First insight into microbiome profile of fungivorous thrips *Hoplothrips carpathicus* (Insecta: Thysanoptera) at different developmental stages: molecular evidence of *Wolbachia* endosymbiosis. *Sci Rep-UK* 2018; 8 (1): 14376.

Kolasa M, Ścibior R, Mazur MA, *et al*. How hosts taxonomy, trophy, and endosymbionts shape microbiome diversity in beetles. *Microb Ecol* 2019; 1-19.

Kondo N, Shimada M, Fukatsu T. Infection density of *Wolbachia* endosymbiont affected by co-infection and host genotype. *Biol Letters* 2005; 1: 488–491.

Kurtz ZD, Müller CL, Miraldi ER, *et al*. Sparse and compositionally robust inference of microbial ecological networks. *PLoS Comput Biol* 2015; 11 (5): e1004226.

Martinson VG, Douglas AE, Jaenike J. Community structure of the gut microbiota in sympatric species of wild *Drosophila*. *Ecol Letters* 2017; 20 (5): 629-639.

Mazza G, Chouaia B, Lozzia GC, *et al*. The bacterial community associated to an italian population of *Psacothea hilaris*: a preliminary study. *Bull Insectol* 2014; 67: 281–285.

McFrederick QS, Wcislo WT, Hout MC, *et al*. Host species and developmental stage, but not host social structure, affects bacterial community structure in socially polymorphic bees. FEMS *Microb Ecol* 2014; 88 (2): 398-406.

Minard G, Mavingui P, Moro CV. Diversity and function of bacterial microbiota in the mosquito holobiont. *Parasite Vector* 2013; 6 (1): 146.

Muhammad A, Fang Y, Hou Y, *et al*. The gut entomotype of red palm weevil *Rhynchophorus ferrugineus* Olivier (Coleoptera: Dryophthoridae) and their effect on host nutrition metabolism. *Front Microbiol* 2017; 8: 2291.

Navajas M, Gutierrez J, Lagnel J, *et al*. Mitochondrial cytochrome oxidase I in tetranychid mites: A comparison between molecular phylogeny and changes of morphological and life history traits. *Bull Ent Res* 1996; 86(4): 407–417.

Oliver KM, Russell JA, Moran NA, *et al*. Facultative bacterial symbionts in aphids confer resistance to parasitic wasps. *P Natl Acad Sci USA* 2003; 100: 1803–1807.

Pollock J, Glendinning L, Wisedchanwet T, *et al*. The madness of microbiome: attempting to find consensus "best practice" for 16S microbiome studies. *Appl Environ Microbiol* 2018; 84(7): e02627-17.

Pornwiroon W, Kearney MT, Husseneder C, *et al*. Comparative microbiota of *Rickettsia* felis-uninfected and -infected colonized cat fleas, *Ctenocephalides felis*. *ISME J* 2007; 1: 394–402.

R Development Core Team. R: A Language and Environment for Statistical Computing. R Foundation for Statistical Computing, Vienna, Austria. URL. 2016.

Sazama EJ, Ouellette SP, Wesner JS. Bacterial endosymbionts are common among, but not necessarily within, insect species. *Environ Entomol* 2019; 48(1): 127–133.

Scarborough CL, Ferrari J, Godfray HCJ. Aphid protected from pathogen by endosymbiont. *Science* 2005; 310: 1781.

Staudacher H, Schimmel BC, Lamers MM, *et al*. Independent effects of a herbivore's bacterial symbionts on its performance and induced plant defences. *Int J Mol Sci* 2017; 18: 182.

Tchioffo MT, Boissière A, Abate L, *et al*. Dynamics of bacterial community composition in the malaria mosquito's epithelia. *Front Microbiol* 2016; 6:1500.

Thapa S, Zhang Y, Allen MS. Effects of temperature on bacterial microbiome composition in *Ixodes scapularis* ticks. *MicrobiologyOpen* 2018; e00719.

Turelli M, Hoffmann AA. Rapid spread of an inherited incompatibility factor in California *Drosophila*. *Nature* 1991; 353 (6343): 440.

Wang J, Chung SH, Peiffer M, *et al*. Herbivore oral secreted bacteria trigger distinct defense responses in preferred and non-preferred host plants. *J Chem Ecol* 2016; 42 (6): 463-474.

Walter DE, Proctor HC. Mites: ecology, evolution and behaviour. CABI Publishing, 1999.

Zélé F, Santos I, Olivieri I, *et al*. Endosymbiont diversity and prevalence in herbivorous spider mite populations in South-Western Europe. *FEMS Microbiol Ecol* 2018a; 94: 015.

Zélé F, Santos JL, Godinho DP, *et al*. *Wolbachia* both aids and hampers the performance of spider mites on different host plants. *FEMS Microbiol Ecol* 2018b; fiy187.

Zhang YK, Chen YT, Yang K, *et al*. Screening of spider mites (Acari: Tetranychidae) for reproductive endosymbionts reveals links between co-infection and evolutionary history. *Sci Rep-UK* 2016; 6: 27900.

Zhang YK, Yang K, Zhu YX, *et al*. Symbiont-conferred reproduction and fitness benefits can favour their host occurrence. *Ecol Evol* 2018; 8(3): 1626–1633.

Zhou J, He Z, Yang Y, *et al*. High-throughput metagenomic technologies for complex microbial community analysis: open and closed formats. *MBio* 2015; 6(1): e02288-14.

Zhu YX, Song YL, Hoffmann AA, *et al*. A change in the bacterial community of spider mites decreases fecundity on multiple host plants. *MicrobiologyOpen* 2019a; 8(6): e00743.

Zhu YX, Song YL, Zhang YK, *et al*. Incidence of facultative bacterial endosymbionts in spider mites associated with local environment and host plant. *Appl Environ Microb* 2018; 84: e02546-17.

Zhu YX, Song ZR, Song YL, *et al.* The microbiota in spider mite faeces potentially reflects intestinal bacterial communities in the host. *Insect Sci* 2019b.

Zouache K, Raharimalala FN, Raquin V, *et al*. Bacterial diversity of field-caught mosquitoes, *Aedes albopictus* and *Aedes aegypti*, from different geographic regions of Madagascar. *FEMS Microbiol Ecol* 2011; 75(3): 377-389.

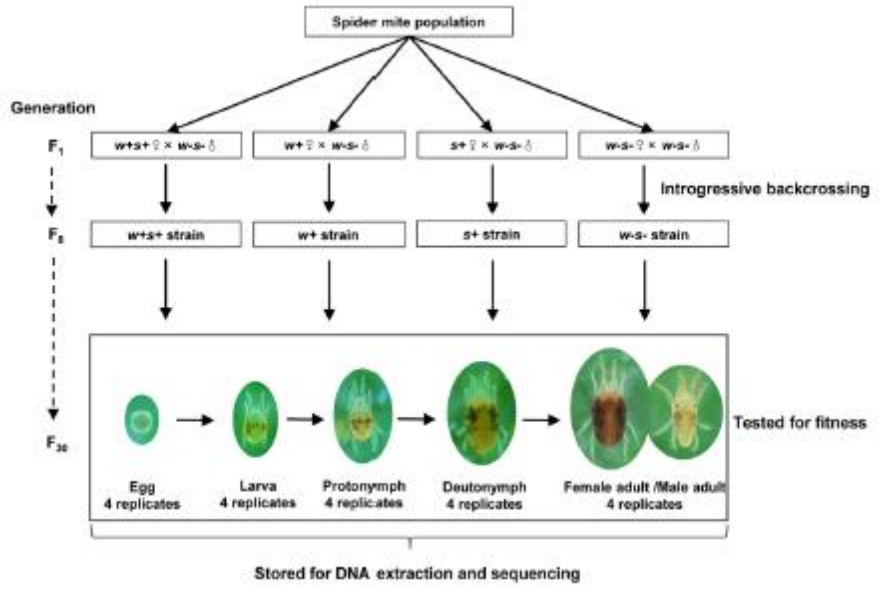

Figure 1. Overview of the experimental procedure. The photos of the spider mite (*T. truncatus*) at different developmental stages were taken with a Leica camera (DVM6a). *w+s+*, *w+*, *s+*, and *w-s-* represent the spider mite strains infected with both *Wolbachia* and *Spiroplasma*, only *Wolbachia*, only *Spiroplasma*, and no endosymbionts, respectively.

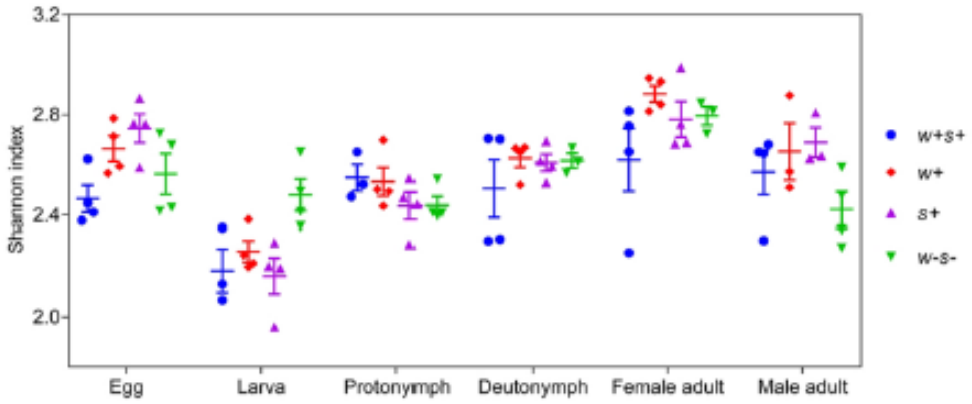

Figure 2. Shannon index values of the bacterial communities from four spider mite strains at different developmental stages. Data are shown as the mean ± SEM. *w*+*s*+, *w*+, *s*+, and *w*-*s*- represent the four spider mite strains as described in the caption for Fig. 1.

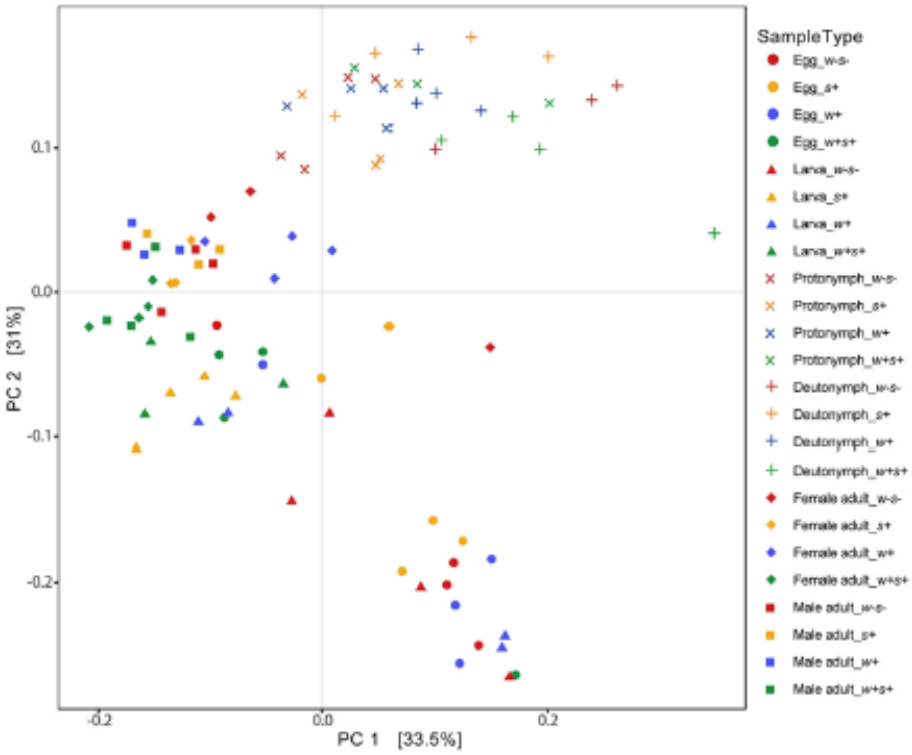

Figure 3. Principal coordinates analysis (PCoA) plot based on the Bray-Curtis distance matrix representing differences in the composition of the microbiota from the four spider mite (*T. truncatus*) strains at different developmental stages. The variation explained by the PCoA axes is given in parentheses. Different colors represent different samples. *w*+*s*+, *w*+, *s*+, and *w*-*s*- represent the four spider mite strains as described in the caption for Fig. 1.

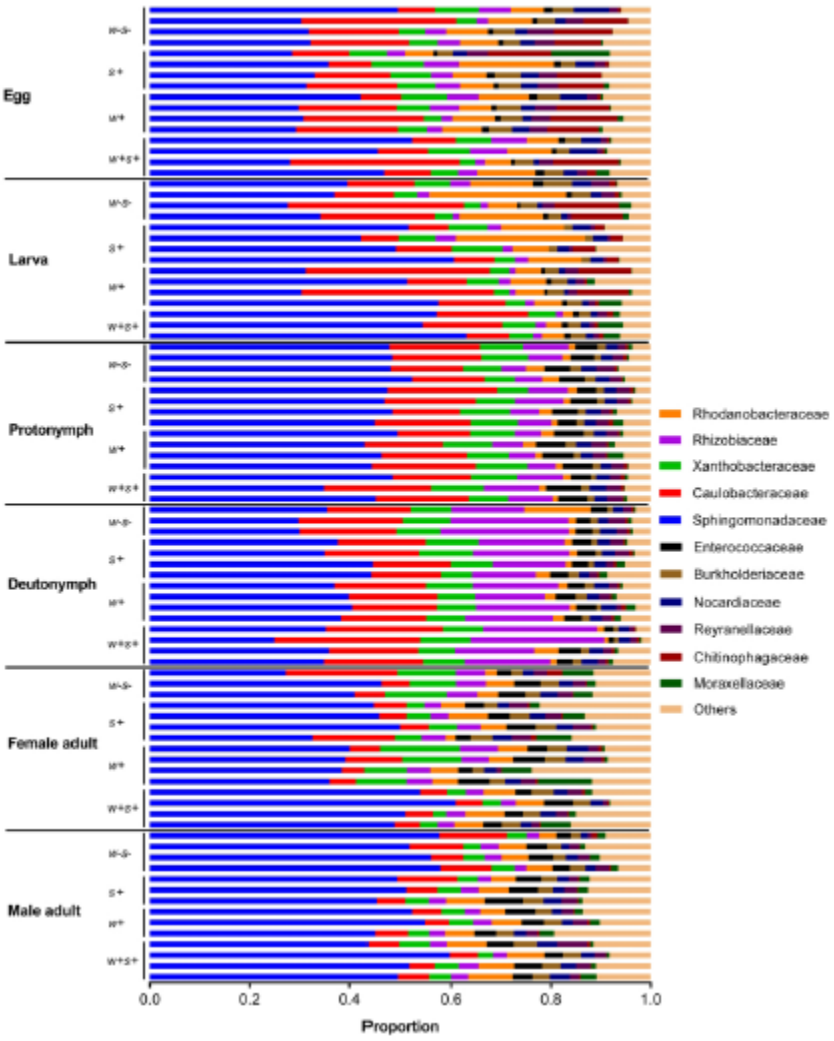

Figure 4. Class-level bacterial community composition in the four spider mite (*T. truncatus*) strains at different developmental stages, assessed with Illumina 16S rRNA amplicon-sequencing. *w+s+*, *w+*, *s+*, and *w-s-* represent the four spider mite strains as described in the caption for Fig. 1.

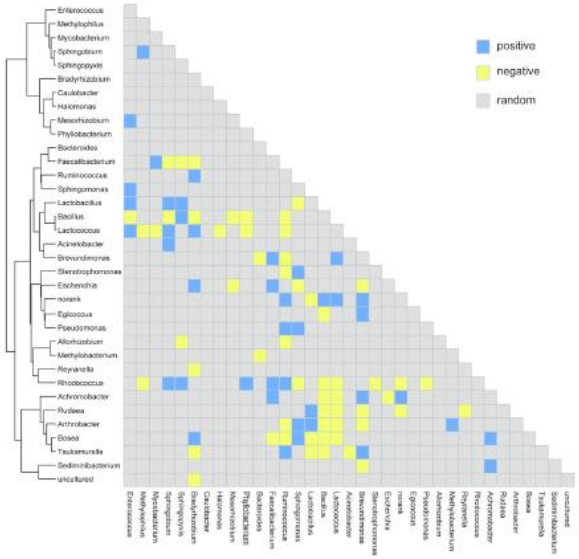

Figure 5. Pairwise cooccurrence patterns between the bacterial OTUs in the four spider mite strains at different developmental stages. Each tick on the x- and y-axis refers to an OTU. Blue, yellow, and gray squares indicate positive, negative and random cooccurrences between two OTUs, respectively.

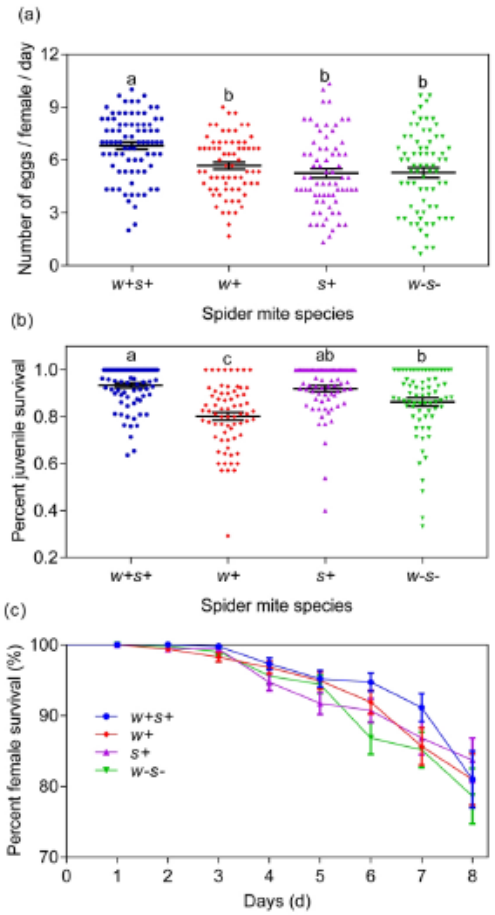

Figure 6. Performance of the four spider mite (*T. truncatus*) strains. (a) Daily fecundity; (b) juvenile survival rate; (c) female survival rate. Data are shown as the mean ± SEM. Different letters above the strains indicate a significant difference at a level of $P < 0.05$. *w+s+*, *w+*, *s+*, and *w-s-* represent the four spider mite strains as described in the caption for Fig. 1.

Table 1. Effects on the variation in the microbiota α-diversity (Shannon index).

Factor	LR *Chi-square*	*df*	*P*-value
Endosymbiont	10.254	3	0.016
DS (Developmental stage*sex)	112.515	5	< 0.001
Endosymbiont × DS (Developmental stage*sex)	33.791	15	0.004

Table 2 Main function analysis of the microbiomes present in four spider mite (*T. truncatus*) strains at different developmental stages.

Developmental stage	KEGG category	ID	KEGG description	Ko abundance (Mean% ± SEM)				Kruskal-Wallis test		
				w+s+	*w+*	*s+*	*w-s-*	*Chi-square*	*df*	*P*
Egg	Staurosporine biosynthesis	K14266	FADH2 O2-dependent halogenase I	0.26 ± 0.04	0.18 ± 0.02	0.19 ± 0.03	0.22 ± 0.02	2.63	3	0.45
	Genetic information processing	K03088	RNA polymerase sigma-70 factor, ECF subfamily	0.59 ± 0.08	0.46 ± 0.04	0.51 ± 0.08	0.51 ± 0.03	2.23	3	0.53
		K02529	LacI family transcriptional regulator	0.30 ± 0.04	0.22 ± 0.02	0.25 ± 0.04	0.25 ± 0.01	3.31	3	0.35
		K03704	Cold shock protein (beta-ribbon, CspA family)	0.23 ± 0.03	0.18 ± 0.01	0.21 ± 0.03	0.19 ± 0.01	3.38	3	0.34
	Lipid metabolism	K00059	3-oxoacyl-[acyl-carrier protein] reductase	0.35 ± 0.04	0.27 ± 0.02	0.32 ± 0.05	0.30 ± 0.01	3.22	3	0.36
	Signal transduction	K03406	Methyl-accepting chemotaxis protein	0.61 ± 0.07	0.44 ± 0.03	0.50 ± 0.07	0.51 ± 0.03	4.08	3	0.25
	Glutathione metabolism	K00799	Glutathione S-transferase	0.54 ± 0.06	0.40 ± 0.03	0.50 ± 0.07	0.45 ± 0.02	3.73	3	0.29
	Membrane transport	K01999	Branched-chain amino acid transport system substrate-binding protein	0.30 ± 0.06	0.26 ± 0.03	0.37 ± 0.05	0.26 ± 0.04	3.26	3	0.35
	Carbohydrate metabolism	K00626	Acetyl-CoA C-acetyltransferase	0.27 ± 0.03	0.21 ± 0.02	0.25 ± 0.03	0.24 ± 0.01	2.45	3	0.48
	Signaling and cellular processes	K02014	Iron complex outermembrane recepter protein	0.78 ± 0.09	0.57 ± 0.03	0.64 ± 0.09	0.65 ± 0.03	4.08	3	0.25
		K06147	ATP-binding cassette, subfamily B, bacterial	0.25 ± 0.03	0.19 ± 0.02	0.23 ± 0.03	0.20 ± 0.01	3.26	3	0.35
Larva	Staurosporine	K14266	FADH2 O2-dependent	0.34 ±	0.41 ± 0.02	0.24 ±	0.30 ±	8.88	3	**0.03**

	biosynthesis		halogenase I	0.03		0.03	0.03			
	Genetic information processing	K03088	RNA polymerase sigma-70 factor, ECF subfamily	0.66 ± 0.06	0.80 ± 0.04	0.52 ± 0.05	0.66 ± 0.07	6.42	3	0.09
		K02529	LacI family transcriptional regulator	0.33 ± 0.02	0.39 ± 0.01	0.27 ± 0.03	0.31 ± 0.03	8.72	3	**0.03**
	Lipid metabolism	K00059	3-oxoacyl-[acyl-carrier protein] reductase	0.39 ± 0.02	0.42 ± 0.02	0.31 ± 0.03	0.37 ± 0.05	6.34	3	0.1
	Signal transduction	K03406	Methyl-accepting chemotaxis protein	0.85 ± 0.05	0.89 ± 0.02	0.60 ± 0.08	0.68 ± 0.07	8.65	3	**0.03**
	Glutathione metabolism	K00799	Glutathione S-transferase	0.68 ± 0.03	0.69 ± 0.03	0.49 ± 0.05	0.58 ± 0.07	7.09	3	0.07
	Carbohydrate metabolism	K00626	Acetyl-CoA C-acetyltransferase	0.32 ± 0.02	0.36 ± 0.00	0.22 ± 0.02	0.30 ± 0.04	8.6	3	**0.04**
	Membrane transport	K01999	Branched-chain amino acid transport system substrate-binding protein	0.29 ± 0.02	0.28 ± 0.05	0.26 ± 0.02	0.29 ± 0.08	0.93	3	0.82
	Signaling and cellular processes	K02014	Iron complex outermembrane recepter protein	1.11 ± 0.05	1.14 ± 0.05	0.74 ± 0.10	0.89 ± 0.08	9.38	3	**0.02**
		K06147	ATP-binding cassette, subfamily B, bacterial	0.27 ± 0.01	0.28 ± 0.02	0.31 ± 0.03	0.24 ± 0.04	2.87	3	0.41
Protonymph	Staurosporine biosynthesis	K14266	FADH2 O2-dependent halogenase I	0.25 ± 0.04	0.23 ± 0.02	0.31 ± 0.03	0.23 ± 0.02	5.02	3	0.17
	Genetic information processing	K03088	RNA polymerase sigma-70 factor, ECF subfamily	0.65 ± 0.11	0.56 ± 0.04	0.73 ± 0.05	0.54 ± 0.05	5.56	3	0.14
		K02529	LacI family transcriptional regulator	0.34 ± 0.05	0.28 ± 0.02	0.36 ± 0.03	0.27 ± 0.03	5.98	3	0.11
	Lipid metabolism	K00059	3-oxoacyl-[acyl-carrier protein] reductase	0.37 ± 0.06	0.32 ± 0.02	0.41 ± 0.03	0.31 ± 0.03	6.48	3	0.09
	Signal transduction	K03406	Methyl-accepting chemotaxis protein	0.59 ± 0.09	0.56 ± 0.05	0.73 ± 0.06	0.54 ± 0.05	5.64	3	0.13

	Glutathione metabolism	K00799	Glutathione S-transferase	0.59 ± 0.09	0.52 ± 0.04	0.67 ± 0.05	0.50 ± 0.05	5.65	3	0.13
	Membrane transport	K01999	Branched-chain amino acid transport system substrate-binding protein	0.35 ± 0.06	0.30 ± 0.02	0.36 ± 0.03	0.26 ± 0.03	5.66	3	0.13
	Carbohydrate metabolism	K00626	Acetyl-CoA C-acetyltransferase	0.32 ± 0.05	0.28 ± 0.02	0.35 ± 0.02	0.26 ± 0.03	5.39	3	0.15
	Signaling and cellular processes	K02014	Iron complex outermembrane recepter protein	0.79 ± 0.11	0.75 ± 0.06	0.95 ± 0.08	0.72 ± 0.07	5.24	3	0.15
		K06147	ATP-binding cassette, subfamily B, bacterial	0.29 ± 0.04	0.24 ± 0.02	0.31 ± 0.02	0.24 ± 0.02	5.52	3	0.14
Deuton ymph	Genetic information processing	K03088	RNA polymerase sigma-70 factor, ECF subfamily	1.17 ± 0.10	1.21 ± 0.15	1.29 ± 0.13	1.50 ± 0.19	3.39	3	0.34
	Glutathione metabolism	K00799	Glutathione S-transferase	1.02 ± 0.09	1.07 ± 0.14	1.15 ± 0.11	1.36 ± 0.16	3.58	3	0.31
	Signal transduction	K03406	Methyl-accepting chemotaxis protein	0.89 ± 0.07	0.98 ± 0.13	1.07 ± 0.10	1.11 ± 0.08	2.94	3	0.4
	Signaling and cellular processes	K02014	Iron complex outermembrane recepter protein	1.14 ± 0.09	1.29 ± 0.16	1.39 ± 0.13	1.45 ± 0.10	3.11	3	0.37
Female adult	Genetic information processing	K03088	RNA polymerase sigma-70 factor, ECF subfamily	0.79 ± 0.24	0.67 ± 0.07	0.69 ± 0.02	0.76 ± 0.06	0.76	3	0.86
		K02529	LacI family transcriptional regulator	0.32 ± 0.05	0.32 ± 0.03	0.32 ± 0.01	0.35 ± 0.02	1.36	3	0.71
	Lipid metabolism	K00059	3-oxoacyl-[acyl-carrier protein] reductase	0.35 ± 0.03	0.43 ± 0.05	0.41 ± 0.02	0.48 ± 0.03	5.23	3	0.16
	Signal transduction	K03406	Methyl-accepting chemotaxis protein	0.56 ± 0.03	0.63 ± 0.08	0.72 ± 0.06	0.80 ± 0.08	5.91	3	0.12
	Glutathione metabolism	K00799	Glutathione S-transferase	0.46 ± 0.02	0.64 ± 0.09	0.60 ± 0.04	0.76 ± 0.05	7.37	3	0.06
	Membrane transport	K01999	Branched-chain amino acid transport system substrate-binding	0.21 ± 0.00	0.54 ± 0.09	0.34 ± 0.02	0.55 ± 0.01	11.18	3	**0.01**

			protein							
	Signaling and cellular processes	K02014	Iron complex outermembrane recepter protein	0.87 ± 0.07	0.82 ± 0.09	0.94 ± 0.08	1.03 ± 0.11	3.19	3	0.36
	Signaling and cellular processes	K06147	ATP-binding cassette, subfamily B, bacterial	0.34 ± 0.05	0.36 ± 0.03	0.32 ± 0.02	0.39 ± 0.02	2.65	3	0.45
	Carbohydrate metabolism	K00626	Acetyl-CoA C-acetyltransferase	0.24 ± 0.02	0.33 ± 0.04	0.32 ± 0.01	0.37 ± 0.03	7.15	3	0.07
Male adult	Genetic information processing	K03088	RNA polymerase sigma-70 factor, ECF subfamily	0.66 ± 0.07	0.66 ± 0.08	0.68 ± 0.08	0.78 ± 0.11	0.61	3	0.89
		K02529	LacI family transcriptional regulator	0.32 ± 0.04	0.33 ± 0.05	0.32 ± 0.03	0.38 ± 0.05	1.03	3	0.79
	Lipid metabolism	K00059	3-oxoacyl-[acyl-carrier protein] reductase	0.41 ± 0.05	0.40 ± 0.06	0.39 ± 0.04	0.45 ± 0.06	0.57	3	0.9
	Signal transduction	K03406	Methyl-accepting chemotaxis protein	0.72 ± 0.10	0.74 ± 0.11	0.70 ± 0.05	0.90 ± 0.14	1.68	3	0.64
	Glutathione metabolism	K00799	Glutathione S-transferase	0.60 ± 0.08	0.61 ± 0.10	0.58 ± 0.04	0.71 ± 0.11	1.57	3	0.67
	Carbohydrate metabolism	K00626	Acetyl-CoA C-acetyltransferase	0.30 ± 0.04	0.31 ± 0.04	0.31 ± 0.03	0.35 ± 0.05	1.19	3	0.75
	Membrane transport	K01999	Branched-chain amino acid transport system substrate-binding protein	0.31 ± 0.03	0.31 ± 0.05	0.29 ± 0.03	0.29 ± 0.04	0.61	3	0.89
	Signaling and cellular processes	K02014	Iron complex outermembrane recepter protein	0.95 ± 0.14	0.97 ± 0.15	0.94 ± 0.07	1.19 ± 0.18	1.68	3	0.64
		K06147	ATP-binding cassette, subfamily B, bacterial	0.37 ± 0.04	0.35 ± 0.05	0.32 ± 0.03	0.35 ± 0.04	1.01	3	0.8

Note that analyses with significant effects are highlighted in bold. *w+s+*, *w+*, *s+*, and *w-s-* represent the four spider mite strains as described in the caption for Fig. 1.